Catalytic Activity, Surface Redox Properties, and Structural Evolution during the Thermal Processing of Chromium-Promoted Ceria Oxidation Catalysts

Philip G. Harrison* and Wayne Daniell†

Department of Chemistry, University of Nottingham, University Park, Nottingham NG7 2RD, United Kingdom

Received October 9, 2000. Revised Manuscript Received January 10, 2001

Chromium-promoted ceria catalyst materials have been prepared by three routes: impregnation of ceria gel using an aqueous solution of CrO_3 (Cr(VI)/CeO_2-imp), impregnation of ceria gel using an aqueous solution of chromium(III) nitrate (Cr(III)/CeO_2-imp), and coprecipitation from an aqueous solution containing both chromium(III) nitrate and cerium(III) nitrate (Cr(III)/CeO_2-cop). Optimum catalytic performance toward the oxidation of carbon monoxide and propane is achieved after thermal activation in air in the temperature range 573−673 K. After such treatment the catalytic activity is similar, irrespective of whether the source of the chromium promoter is in oxidation state of 3+ or 6+. Thermal treatment at more elevated temperatures results in a progressive lowering of activity, although 100% conversion of propane is still achieved even after calcination at 1273 K. Examination of the nature of the materials by powder X-ray diffraction (XRD), Fourier transform infrared (FTIR), Fourier transform Raman (FT-Raman), electron paramagnetic resonance (EPR), and X-ray near-edge absorption (XANES) spectroscopies show that the nature of the catalysts formed by thermal processing of the initial materials formed by all three routes in the temperature range 573−673 K is essentially the same. The active catalyst appears to be a composite oxide material comprising microparticulate mixed-valence chromium oxide, possibly Cr_5O_{12}, and Cr(III) oxide-like clusters dispersed on particulate ceria. Thermal processing at ≥873 K results in an increase of particle size and phase separation of Cr_2O_3. In situ EPR studies demonstrate that the mixed-valence component of the catalyst undergoes facile reduction upon exposure to carbon monoxide at 473−573 K and is reoxidized upon exposure to oxygen at the same temperature.

Introduction

Supported chromium oxide catalysts have been of significant industrial importance for many decades and are now vital the polymerization of ethylene (in the manufacture of high-density polymers)[1] as well as the generation of valuable alkenes via the dehydrogenation of low-cost alkane feedstocks.[2] This industrial significance has triggered a vast amount of research into many aspects of their catalytic performance[3,4] and the determination of their active species through both spectroscopic and gravimetric means.[5,6] However, although this research has generated much useful data, it has at the same time raised a great deal of controversy over a number of fundamental characteristics of the supported chromia systems. Among these, two points remain the focus of continuing debate: (i) the physicochemical identity of the Cr−O surface species and (ii) the catalytically active oxidation state of chromium. Of the few accepted conclusions to as yet come out of these discussions, it is generally agreed that these characteristics are strongly influenced by (a) the chromium content of the system, (b) the pretreatment conditions, and (c) the nature of the support material employed.

Aside from the well-known silica and alumina supports, attention has been paid to zirconia-supported chromia (for the dehydrogenation of propane)[7] and to chromia−titania catalysts for the selective catalytic reduction of NO using NH_3.[8] More recently, cerium-oxide-supported chromia catalysts have been used for the oxidative dehydrogenation of isobutane[9] where the activity of these materials was attributed to dispersed $Cr^{6+}O_x$ species.[10] Increased Cr coverage initially led to increased activity, but was followed by the appearance

* To whom correspondence should be addressed.
† Present address: Institut fuer Physikalische Chemie, Ludwig Maximilians Universitaet Muenchen, Butenandtstr. 5-13, 81377 Muenchen, Germany.

(1) McDaniel, M. P. *Adv. Catal.* **1985**, *33*, 47.
(2) Poole, C. P.; MacIver, D. S. *Adv. Catal.* **1967**, *17*, 223.
(3) Weckhuysen, B. M.; Wachs, I. E.; Schoonheydt, R. A. *Chem. Rev.* **1996**, *96*, 3327.
(4) Weckhuysen, B. M.; Schoonheydt, R. A. *Catal. Today* **1999**, *51*, 223.
(5) Zaki, M. I.; Fouad, N. E.; Leyrer, J.; Knözinger, H. *Appl. Catal.* **1986**, *21*, 359.
(6) Fouad, N. E.; Knözinger, H.; Zaki, M. I.; Mansour, S. A. S. *Z. Phys. Chem.* **1991**, *171*, 75.
(7) De Rossi, S.; Ferraris, G.; Fremiotti, Cimino, A.; Indovina, V. *Appl. Catal. A* **1992**, *81*, 113.
(8) Schneider, H.; Scharf, U.; Wokaun, A.; Baiker, A. *J. Catal.* **1994**, *147*, 545.
(9) Moriceau, P.; Grzybowska, B.; Barbaux, Y.; Wrobel, G.; Hecquet, G. *Appl. Catal. A* **1998**, *168*, 269.
(10) Moriceau, P.; Grzybowska, B.; Gengembre, L.; Barbaux, Y. *Appl. Catal. A* **2000**, *199*, 73.

10.1021/cm001193s CCC: $20.00
Published on Web 04/13/2001

of dispersed Cr^{3+} species and then agglomerated Cr_2O_3, which hindered any further increase. Tin-oxide-supported chromia catalysts have been reported as displaying very promising activity as two-way and three-way exhaust gas catalysts,[11] and recent papers[12,13] have investigated the nature of the Cr sites in relation to the thermal pretreatment and preparation procedure. It is proposed that pretreatment at 573 K generates a mixed-valence Cr(III/VI) species that is responsible for the observed activity. Similar conclusions were reported for methane oxidation over Cr/Al_2O_3 catalysts.[14]

In this paper we focus on the use of cerium(IV) oxide (ceria) as a support for chromia, a system that has so far received very little attention.[15] Ceria is well-known as a component in modern three-way exhaust gas catalysts[16] in which it serves a variety of functions. Primarily, it acts as an oxygen reservoir, being able to release oxygen from its lattice under fuel-rich conditions and store oxygen under lean conditions. This is achieved via the facile $Ce^{3+}-Ce^{4+}$ redox couple and the presence of oxygen defects within the fluorite structure.[17] Second, ceria is also known to stabilize the dispersion of the active metal components.[18]

To assess the suitability of ceria-supported chromia as an exhaust gas catalyst, the activity of coprecipitated (Cr^{III} precursor) and impregnated (Cr^{III} and Cr^{VI} precursors) materials toward CO and propane oxidation has been investigated. The materials were calcined at temperatures in the range 573−1273 K and examined using powder XRD, FTIR, EPR, and XANES spectroscopies, with the aim of establishing a relationship between the preparation procedure/thermal treatment and (i) the nature of the surface chromium species generated and (ii) the observed catalytic activity of these species.

Experimental Section

Catalyst Preparation. Chromium-promoted ceria catalyst materials were prepared by three routes.

(1) By Impregnation of Ceria Gel Using an Aqueous Solution of CrO_3. To a vigorously stirred solution of CrO_3 (80 dm^{-3}, 1.00 M) was added ceria powder (5 g obtained by the ammonia precipitation method). This suspension was stirred for 18 h, cooled to room temperature, and filtered (but not washed) at water pump pressure. The yellow solid was dried overnight at 333 K and is referred to as Cr(VI)/CeO_2-imp with the Cr:Ce atomic ratio in parentheses. The effect of the chromium concentration in solution on the final chromium content of the catalyst was investigated in a similar fashion by using chromic acid solutions ranging in molarity from 0.06 to 2.00 mol dm^{-3} to impregnate portions (5 g) of freshly prepared ceria. The final chromium loading in the catalysts [%Cr] is related to the chromium molarity [M] in solution in the molarity range 0.06−1.00 M by the expression

$$[\%Cr] = 6.453 - 0.283\,[M]^{-1}$$

with a correlation coefficient of $R^2 = 0.995$. Above a molarity of 1.00 M the chromium loading on the catalyst is greater than expected from this expression.

(2) By Impregation of Ceria Gel Using an Aqueous Solution of Chromium(III) Nitrate. Dried (333 K, 12 h) ceria (5 g) was slurried in a solution of $Cr(NO_3)_3 \cdot 9H_2O$ in triply distilled water (50 dm^{-3}) and stirred at room temperature overnight. The pale green solid was filtered off and dried at 333 K for 12 h. This catalyst material is referred to as Cr(III)/CeO_2-imp with the Cr:Ce atomic ratio in parentheses.

(3) By Coprecipitation from an Aqueous Solution Containing Both Chromium(III) Nitrate and Cerium(III) Nitrate. The mixed hydroxide gel was precipitated by the dropwise addition of aqueous ammonia/hydrogen peroxide over a period of 1 h, and after the solution was stirred overnight, the precipitate was washed with triply distilled water and centrifuged five times. The dark brown solid was dried overnight at 383 K in air. This catalyst material is referred to as Cr(III)/CeO_2-cop with the Cr:Ce atomic ratio in parentheses.

Catalyst Thermal Pretreatment. Chromium-promoted ceria catalyst materials (approximately 2-g aliquots) were calcined in an alumina boat for 24 h using a Vecstar 91e tube furnace at temperatures in the range 333−1273 K. Samples became initially dark green and then black at 1273 K.

Physical and Spectroscopic Measurements. X-ray fluorescence (XRF) data were kindly obtained by LSM Ltd., Rotherham, using a Philips PW1480 wavelength dispersive instrument. Samples were prepared as a 10% dilution in a lithium tetraborate bead. Infrared spectra were obtained from KBr disk samples using a Nicolet 20SXC spectrometer. Thirty-two scans were recorded for each sample at a resolution of 1 cm^{-1}. FT-Raman spectra were recorded using a Perkin-Elmer 2000 NIR FT-Raman spectrometer equipped with a Nd^{3+} YAG laser and controlled by GRAMS software. Between 32 and 64 scans at 8-cm^{-1} resolution were accumulated per spectrum with laser power settings of 50−250 mW. With darker colored materials, KBr powder was mixed in with the sample to serve as a diluent.

EPR measurements were recorded at 77 K using a Bruker EMX EPR spectrometer equipped with a Bruker ER 041 XG Microwave bridge in X-band at ca. 9.2 GHz. Experimental g values were determined with reference to diphenyl picryl hydrazyl (DPPH) ($g = 2.0036$). Samples were accurately weighed, 68 ± 2 mg being used, packed into quartz tubes (5 mm), and allowed to equilibrate at 77 K in the resonant cavity before scanning. Semiquantification of the spectra was performed by double integration of the baseline-corrected spectra and comparison with a DPPH reference. No simulated spectra were run. The intensity of the signal was measured by calculating the area under the main peak ($g_\perp = 1.968$, $g_\parallel = 1.936$).

Powder X-ray diffraction data were acquired using a Philips X-pert system fitted with a PW 1710 diffractometer control unit with Cu Kα radiation ($\lambda = 1.5405$ Å). Representative diffractograms were acquired over 5°−80° 2θ with 0.02° steps and 0.4 s acquisition times per step. DICVOL91[19] was used for indexing the diffractograms. Phase identification was corroborated by comparison to the JCPDS database.[20] Particle sizes were calculated using the Scherrer equation.

Cr K-edge (5989.2 eV) X-ray absorption spectra were performed on a station 8.1 at the Daresbury Laboratory, Warrington, U.K, which operates at an energy of up to 2.0 GeV and a maximum beam current of 200 mA. The recording of EXAFS spectra was not possible due to interference from Ce L_{II}-edge (6164.2 eV). Hence, the study was confined to monitoring the changes occurring within the Cr species by observing pre-edge features in the XANES region. A Si(111) double-crystal monochromator was used to select a single-wavelength beam of X-rays; the tuneable energy range that can be

(11) Harrison, P. G.; Harris, U.S. Patent, 4,908,192, 1990.
(12) Harrison, P. G.; Lloyd, N. C.; Daniell, W. *J. Phys. Chem. B* **1998**, *102*, 10672.
(13) Harrison, P. G.; Lloyd, N. C.; Daniell, W.; Bailey, C.; Azelee, W. *Chem. Mater.* **1999**, *11*, 896.
(14) Park, P. W.; Ledford, J. S. *Langmuir* **1997**, *13*, 2726.
(15) Viswanath, R. P.; Wilson, P. *Appl. Catal. A* **2000**, *201*, 23.
(16) Trovarelli, A. *Catal. Rev.−Sci. Eng.* **1996**, *38*, 439.
(17) Zamar, F.; Trovarelli, A.; de Leitenburg, C.; Dolcetti, G. *J. Chem. Soc., Chem. Commun.* **1995**, 965.
(18) Bozon-Verduraz, F.; Besalem, A. *J. Chem. Soc., Faraday Trans.* **1994**, *90*, 653.
(19) DICVOL91, Boultif, A.; Louer, D. *J. Appl. Crystallogr.* **1991**, *24*, 987.
(20) *Powder Diffraction File: Inorganic Phases*; JCPDS−International Centre for Diffraction Data, American Society of Material Testing, 1991.

achieved using this monochromator is 2−10 keV. Forty to fifty percent of the X-ray beam was rejected to filter out the undesired harmonics while retaining 50−60% of the primary beam intensity.

Controlled Atmosphere Gas-Phase Redox Reactions. Reactions in which the catalyst materials were exposed to controlled atmospheres were carried out using a modified EPR tube with connections to a vacuum line. Gas flow to and from the cell was controlled by a two-tap system connected to the cell by metal screw thread fittings. Gas was passed through the sample using a perforated glass capillary inserted into the powdered sample, ensuring maximum contact between gas and sample. The sample was heated by inserting the tube into a sleeve of heating tape, allowing a maximum temperature of 673 K to be achieved.

Samples were initially exposed to a reducing atmosphere of carbon monoxide and heated for a set length of time. The state of sample reduction was then monitored by recording the EPR spectrum. The pressure of CO was increased until the sample showed signs of reduction indicated by a decrease in intensity of the Cr(III) resonance. The gas pressure and temperature were subsequently increased until reduction was complete. After evacuation of the sample tube, samples were reoxidized in a similar fashion by heating in an oxygen atmosphere.

Catalysis Measurements. Catalytic conversion data for the oxidation of carbon monoxide and propane were obtained using a custom-built horizontal geometry continuous-flow microreactor. The furnace consisted of a stainless steel tube surrounded by a cylindrical stainless steel heating block. The sample tube, which sits inside the stainless steel tube, is made of Pyrex glass 1 cm in diameter with a glass sinter in the middle. The catalyst sample was packed on the inlet side of the sinter, supported by dry silica gel pellets, and held in place with glass wool. The outlet side of the sinter was packed with dry silica gel pellets also held in place with glass wool. Catalyst samples were sieved to a particle size range of 38−63 mm and diluted with silica gel of particle size 100 μm. Samples of 0.5 and 2.0 g of catalyst respectively were used for carbon monoxide and propane conversions. Catalyst samples were activated by preheating in situ in the microreactor at 573 K for 2 h under a flow of air and then allowed to cool also under a flow of air. Catalyst temperatures were measured using a thermocouple located close to the catalyst. Gas flows were controlled by mass flow controllers, and concentrations of gas-phase components were measured using precise integration of characteristic infrared peaks (band envelopes: CO 2230−2006 cm^{-1}, CO_2 2379−2259 cm^{-1}, C_3H_8 3050−2802 cm^{-1}). Compositions of the input gas mixtures were 5.00% CO, 20.00% O_2 (O_2-rich), and 75.00% N_2, 30.00% CO, 15.00% O_2, and 55.00% N_2 (stoichiometric), and 2.5% propane, 20.0% O_2, and 77.5% N_2 (oxygen-rich). An overall flow rate of 100 dm^{-3} min^{-1} was used for both mixtures, corresponding to space velocities of ca. 18 000 h^{-1} (for CO oxidation) and ca. 4500 h^{-1} (for propane oxidation).

Results

Catalytic Activity. (1) Oxidation of Carbon Monoxide. Unpromoted cerium(IV) oxide itself exhibits reasonable activity toward the oxidation of CO under oxygen-rich conditions, with 100% conversion being achieved in all cases except for the 1273 K calcined material, which gave only 45% conversion even at 773 K.[21]

Conversion data for the catalytic oxidation of carbon monoxide over Cr(III)/CeO_2-cop and Cr(VI)/CeO_2-imp materials are listed in Table 1. In all cases, CO_2 was the only product of the reaction. These chromium-promoted ceria materials were on the whole less active toward the stoichiometric oxidation of CO than similar Cu-promoted ceria material.[21] Complete conversion for the stoichiometric oxidation of CO typically occurs around 650 K for the Cr(VI)/CeO_2-imp material dried at 333 K after thermal activation pretreatment in air at 573 K. Increasing chromium content and thermal processing at higher temperatures also gave complete conversion but at somewhat higher temperaures. Comparative conversion plots are shown in Figure 1. The activity of the Cr(III)/CeO_2-cop materials is broadly similar to that observed for the Cr(VI)/CeO_2-imp materials. Catalytic activity again decreases with increasing chromium content, with T_{100} temperatures increasinging by ca. 70° with an increase in Cr:Ce ratio from 0.06 to 0.11.

Table 1. Effect of Preparative Route, Chromium Loading, and Ex Situ Calcination Temperature on the Catalytic Activity of Cr-Promoted Ceria Catalysts toward Stoichiometric CO Oxidation

catalyst/ Cr:Ce atom ratio	calcination temp/K	light-off temp/K	T_{100} (CO) temp/K
	Cr(VI)/CeO_2-imp		
0.04	333	373	648
0.06	333	328	653
0.07	333	318	733
0.07	673	328	703
0.07	873	403	773
	Cr(III)/CeO_2-cop		
0.06	673	398	633 (478[a])
0.06	873	448	683 (528[a])
0.11	383	423	583[a]
0.11	673	423	548[a]
0.11	873	478	593[a]

[a] Temperature at which complete conversion was achieved under O_2-rich conditions.

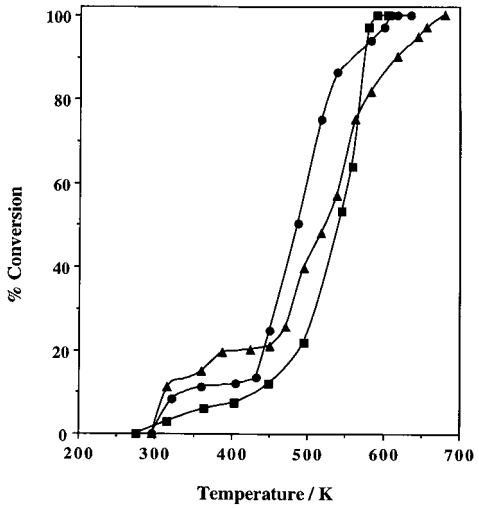

Figure 1. Conversion versus temperature plots for the stoichiometric oxidation of CO over Cr(VI)/CeO_2-imp catalyst materials with Cr:Ce atomic ratios of 0.07 (▲), 0.06 (●), and 0.04 (■).

(2) Oxidation of Propane. Conversion data for the catalytic oxidation of propane over Cr(III)/CeO_2-cop and Cr(VI)/CeO_2-imp materials are listed in Table 2. Only CO_2 and H_2O were produced in all cases. No CO was observed. The temperature at which complete conversion of propane over the Cr(VI)/CeO_2-imp materials dried at 333 K after thermal activation pretreatment in air at 573 K decreased with increasing chromium

(21) Harrison, P. G.; Ball, I. K.; Azelee, W.; Daniell, W.; Goldfarb, D. *Chem. Mater.*, in press.

Table 2. Effect of Preparative Route, Chromium Loading, and Ex Situ Calcination Temperature on the Catalytic Activity of Cr-Promoted Ceria Catalysts toward Propane Oxidation

catalyst/ Cr:Ce atom ratio	calcination temp/K	light-off temp/K	T_{100} (C_3H_8) temp/K
	Cr(VI)/CeO_2-imp		
0.04	333	383	608
0.06	333	343	573
0.07	333	383	553
0.07	673	393	528
0.07	873	423	613
0.07	1273	528	763
	Cr(III)/CeO_2-cop		
0.11	383	438	508
0.11	673	433	493
0.11	873	463	598

loading from 608 K when Cr:Ce = 0.04 to 553 K when Cr:Ce = 0.07, significantly lower values than those for unpromoted ceria (760 K) (Figure 2). However, ex situ thermal processing at 673 K lowered the T_{100} value even further to 528 K. Processing at higher temperatures resulted in the T_{100} value increasing significantly. The Cr(III)/CeO_2-cop material (Cr:Ce 0.11) exhibited even lower T_{100} values (508 K for material dried at 333 K after thermal activation pretreatment in air at 573 K; 493 K after ex situ thermal processing at 673 K). Thermal processing at 873 K again resulted in an increase in the T_{100} value to 598 K.

Fourier Transform Infrared and Raman Spectroscopy. The spectrum of the Cr(VI)/CeO_2-imp (Cr:Ce 0.09) material dried at 333 K is dominated by a series of intense peaks in the Cr=O stretching region at 955, 898−860, and 815 cm^{-1} assigned as the $\nu_{as}(CrO_3)$, $\nu_s(CrO_3)$, and $\nu_{as}(CrOCr)$ vibrations of the adsorbed dinuclear ($Cr_2O_7^{2-}$) chromate species, respectively.[22] The observation of a band at 775 cm^{-1}, however, together with shoulders on the low-wavenumber sides of all other bands, suggests that the adsorbed trinuclear species ($Cr_3O_{10}^{2-}$) may also be present. The sharp, intense peak at 1380 cm^{-1} in both the doped and pure material is due to residual nitrate ions on the ceria surface. Calcination of the material at 573 K reduces the intensity of the bands in the region 1000−750 cm^{-1}, and after thermal treatment at 873 K all bands due to the chromate species are absent and only a broad band at ca. 650 cm^{-1}, indicative of crystalline Cr_2O_3, is present (cf. α-Cr_2O_3 at 635 cm^{-1} [23]).

The FTIR spectra of the Cr(III)/CeO_2-imp (Cr:Ce 0.06) material dried at 333 K and calcined at 573 K are shown in Figure 3. Unlike the analogous Cr(VI)/CeO_2-imp material dried at 333 K, the Cr(III)/CeO_2-imp material (lower trace) shows no Cr=O stretching vibrations. However, calcination at 573 K leads to the formation of two broad bands in the Cr=O stretching region, indicating that partial oxidation of Cr(III) to Cr(VI) has taken place. The two maxima at ca. 930 and 780 cm^{-1} are assigned to $\nu_{as}(CrO_3)$ and $\nu_{as}(CrOCr)$ stretching vibrations of polychromate surface species, respectively. Oxidation of Cr(III) to Cr(VI) has been previously reported by Baker et al.[24] during structural analysis of

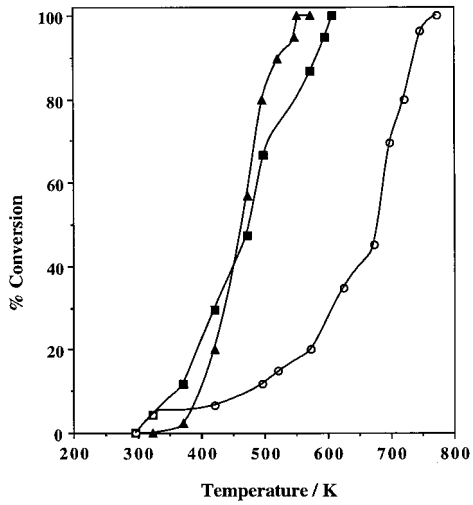

Figure 2. Conversion versus temperature plots for the oxygen-rich oxidation of propane over Cr(VI)/CeO_2-imp catalyst materials with Cr:Ce atomic ratios of 0.07 (▲) and 0.04 (■) and CeO_2 (○).

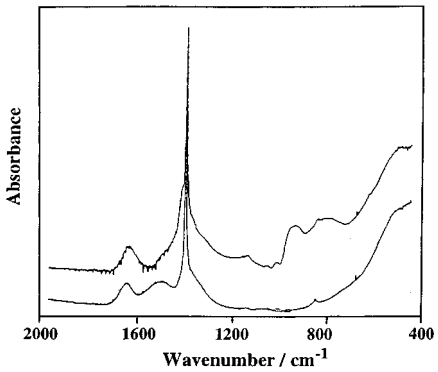

Figure 3. FTIR spectra of Cr(III)/CeO_2-imp (Cr:Ce 0.06) material calcined at 333 K (upper) and 573 K (lower).

hydrated Cr_2O_3 gels and by Scharf et al.[25] in chromium(III)-nitrate-impregnated titania materials. A similar oxidation of chromium(III) to chromium(VI) has been inferred by photoelectron spectroscopy for alumina-supported chromia catalysts.[14] As with the Cr(VI)/CeO_2-imp material, the chromate species present at 573 K are removed by calcination at higher temperatures, resulting in the loss of bands due to chromate and the formation of Cr_2O_3 (peak at ca. 620 cm^{-1}) at 873 K.

Infrared spectra for the Cr(III)/CeO_2-cop (Cr:Ce 0.06) material during calcination at various temperaures in the range 383−1273 K are shown in Figure 4. Unexpectedly, mild thermal processing at 383 K results in the appearance of bands attributable to Cr(VI) species, with the maximum at 950 cm^{-1} assigned to a $\nu_{as}(CrO_3)$ stretching vibration, and bands in the region 890−710 cm^{-1} assigned to various ν(Cr=O) vibrations of polychromate surface ions. The weak band at ca. 1000 cm^{-1}, however, has been attributed to mononuclear Cr(V) species[26] and indicates that complete oxidation to Cr(VI) has not occurred. This observation is not too surprising considering the known surface stabilization of Cr(V).[27] Calcination at 573 K results in a decrease in the

(22) Mattes, R. Z. *Z. Anorg. Allg. Chem.* **1971**, *362*, 163.
(23) Marshall, R.; Mitra, S. S.; Gielisse, P. J.; Mansur, L. C. *J. Chem. Phys.* **1965**, *43*, 2893.
(24) Baker, F. S.; Carruthers, J. D.; Stryker, L. J. *Discuss Faraday Soc.* **1971**, *52*, 173.
(25) Scharf, U.; Schneider, H.; Baiker, A.; Wokaun, A. *J. Catal.* **1994**, *145*, 464.
(26) Schraml-Marth, M.; Wokaun, A.; Baiker, A. *J. Catal.* **1992**, *133*, 415.

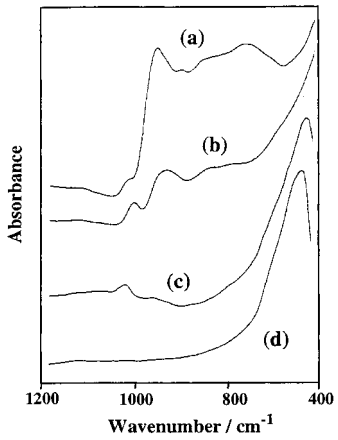

Figure 4. FTIR spectra of Cr(III)/CeO_2-cop (Cr:Ce 0.06) material calcined at (a) 383 K, (b) 573 K, (c) 873 K, and (d) 1273 K.

intensity across the ν(Cr═O) region, with a shift in the peak maximum from 950 to 940 cm^{-1}, suggesting the loss of higher membered polynuclear chromate species. This would indicate that reduction of the polychromate species is occurring at 573 K, leading to their complete removal by 873 K and the formation of Cr_2O_3 (ca. 620 cm^{-1}).

The nature of the Cr(VI)/CeO_2-imp materials may be conveniently studied by FT-Raman spectroscopy. Spectra for materials prepared by exposure of ceria gel to aqueous CrO_3 solutions with Cr concentrations in the range 1.00−2.00 M and dried at 333 K exhibit bands at 965 ($\nu_{as}(CrO_3)$), 876 ($\nu_s(CrO_3)$), 789 (ν_{as}(CrOCr)), and 225 (δ(CrOCr)) cm^{-1} due to adsorbed $Cr_2O_7^{2-}$ ions as well as bands at 904 ($\nu_{as}(CrO_3)$), 837 ($\nu_s(CrO_3)$), and 344 ($\delta(CrO_3)$) cm^{-1} due to adsorbed CrO_4^{2-} ions (Figure 5). Spectra of materials obtained using CrO_3 solutions ≤0.80 M are poorly resolved and exhibit weak bands at ca. 350 and 900 cm^{-1} due to adsorbed CrO_4^{2-} ions. The development of a band at ca. 950 cm^{-1} in the 0.80 M sample indicates that some adsorbed $Cr_2O_7^{2-}$ ions are also present in this material.

Raman band positions are consistent with adsorbed CrO_4^{2-} and $Cr_2O_7^{2-}$ ions.[28] In addition, the band observed at ca. 458 cm^{-1} is due to the CeO_2 support, whereas the band at ca. 688 cm^{-1} is attributed to Cr_2O_3 formed by laser-induced crystallization.[25] The shift of ca. 80 cm^{-1} from the pure, unsupported material is attributed to a support−promoter interaction.[29] Spectra of calcined materials proved on the whole very poor, mainly due to the darker coloration of the samples.

Powder X-ray Diffraction. Diffractograms of the Cr(VI)/CeO_2-imp (Cr:Ce 0.07) material dried after thermal processing in the temperature range 333−1273 K are illustrated in Figure 6. Cr(III)/CeO_2-imp and Cr(III)/CeO_2-cop materials of comparable chromium content gave almost identical diffractograms at each calcination temperature. The diffractogram of the material dried at 333 K exhibits broad, low-intensity peaks characteristic of small crystallites. As the calcination temperature is increased, these peaks become sharper and more intense, reflecting an increase in crystallinity and

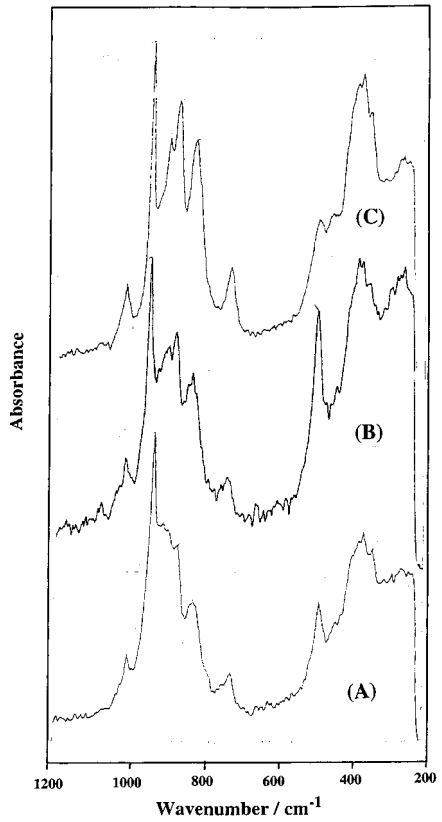

Figure 5. FT-Raman spectra of Cr(VI)/CeO_2-imp catalyst materials dried at 333 K formed by impregnation of CeO_2 with (A) 2.00 M, (B) 1.25 M, and (C) 1.00 M aqueous CrO_3 solutions.

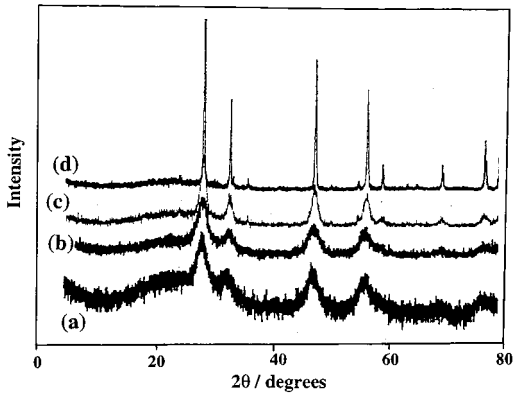

Figure 6. Powder XRD diffractograms of the Cr(VI)/CeO_2-imp (Cr:Ce 0.07) material calcined at temperatures of (a) 333 K, (b) 573 K, (c) 773 K, and 1273 K.

average particle size within the material. By 873 K the cubic pattern of cerium(IV) oxide is identifiable, together with a second, weaker phase. After calcination at 1273 K both sets of peaks sharpen considerably and are identified and indexed by comparison with literature data as CeO_2 and Cr_2O_3.[30,31]

Particle size analysis of the two phases with increasing calcination temperature shows that rapid sintering occurs between 873 and 1273 K. For the ceria phase, average particle sizes were calculated as <10, ca. 10, and 93 nm after calcination at temperatures of 573, 873, and 1273 K, respectively. Phase separation of Cr_2O_3, however, is only detectable after calcination at 873 K,

(27) Cimino, A.; Cordischi, D.; De Rossi, S.; Valigi, M. *J. Catal.* **1991**, *127*, 761.
(28) Michel, G.; Cahay, R. *J. Raman Spectrosc.* **1986**, *17*, 4.
(29) Hardcastle, F. D.; Wachs, I. E. *J. Mol. Catal.* **1988**, *6*, 173.
(30) CeO_2 JCPDS file no. 34-394.
(31) Cr_2O_3 JCPDS file no. 38-1479.

at which stage the average particle size is 14.5 nm, twice that of the ceria support. Calcination at 1273 K resulted in an increase of the Cr_2O_3 crystallites to 101.0 nm. Diffractograms of Cr(VI)/CeO_2-imp materials with different chromium loadings were very similar, with only the relative intensity of the peaks due to Cr_2O_3 varying with the chromium content.

X-ray Absorption Spectroscopy. Although useful EXAFS data could not be accumulated, the nature of the Cr K absorption edge can be unequivocally diagnostic for the presence or otherwise of chromium in the 6+ oxidation state. Chromium 6+ compounds such as $Na_2CrO_4 \cdot 4H_2O$, $Na_2Cr_2O_7 \cdot 2H_2O$, and CrO_3 exhibit an intense pre-edge peak at 4.1−4.3 eV before the edge; however, this feature is absent in chromium(III) compounds such as $Cr_2(SO_4)_3 \cdot 12H_2O$ and $CrK(SO_4)_2 \cdot 12H_2O$.[31] For the Cr^{6+} ion, multiple-scattered-wave calculations have indicated that the pre-edge peak is due to an electronic transition from the Cr 1s orbital to an empty antibonding molecular orbital of primarily Cr 3d character.[32,33] This quadrupole, 1s → 3d, transition is "dipole-allowed" in a tetrahedral ligand field because of the extensive mixing of odd-parity Cr $3d_{z^2}$ and $4p_z$ orbitals with oxygen 2s and $2p_z$ orbitals. The intensity of the 1s → 3d transition varies with the number of d orbital vacancies, the site symmetry of the X-ray absorbing atom, and the metal−ligand bond length.[34] Hence, the observation of a pre-edge feature may be deemed characteristic of chromium in the 6+ oxidation state coordinated tetrahedrally (by oxygen).[35,36]

The Cr K X-ray absorption edge of the Cr(VI)/CeO_2-imp (Cr:Ce 0.06) material after drying at 383 K is illustrated in Figure 7a. As expected for chromium 6+, this material exhibits an intense pre-edge feature that is still present after calcination at 573 K (Figure 7b. However, after calcination at temperatures ≥873 K, the intensity of this feature is greatly reduced (Figure 7c,d), indicative of the reduction of the chromium to the 3+ state. Figure 8 shows a plot of the variation in peak intensity of the pre-edge feature of Cr(VI)/CeO_2-imp materials dried at 383 K with Cr(VI) content and is linear with a high degree of correlation over the range studied (1.8−6.3% Cr).

As expected for a chromium 3+ containing material, no pre-edge feature is observed for the Cr(III)/CeO_2-imp (Cr:Ce 0.06) material dried at 383 K (Figure 9a). However, upon calcination at 573 K, the pre-edge feature was very prominent (Figure 9b) and was still distinct after calcination at 873 K (Figure 9c)) but had disappeared totally after calcination at 1273 K (Figure 9d). This shows unequivocally that although the chromium in the material is totally in the 3+ oxidation state at very low (383 K) and very high (1273 K) thermal treatments, in the mid-temperature range (573−873 K) a substantial part of the chromium content is present in the 6+ oxidation state.

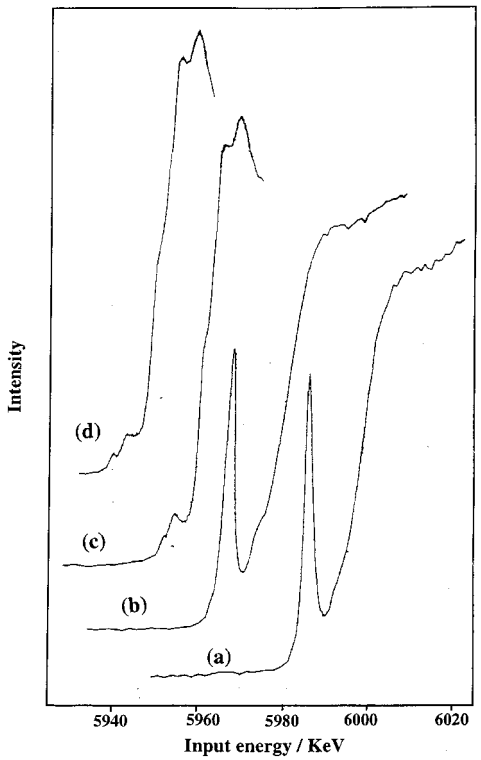

Figure 7. Cr K X-ray absorption edge of the Cr(VI)/CeO_2-imp (Cr:Ce 0.06) material calcined at (a) 383 K, (b) 573 K, (c) 873 K, and (d) 1273 K.

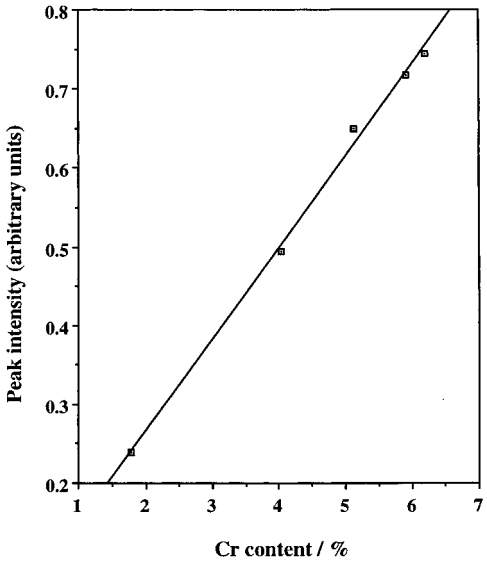

Figure 8. Plot of the variation in peak intensity of the pre-edge feature of Cr(VI)/CeO_2-imp materials with Cr(VI) content. Solid line represents the least-squares best fit ($I = 0.116$[Cr] $+ 0.03R^2 = 0.997$).

In contrast and quite unexpectedly, the absorption edge of the Cr(III)/CeO_2-cop (Cr:Ce 0.06) material exhibited a very strong pre-edge feature even after the mild thermal treatment of drying at 383 K (Figure 10a) and which was essentially unchanged after calcination at 573 K (Figure 10b). The intensity of the pre-edge peak was greatly reduced after calcination at 873 K (Figure 10c) and totally absent after treatment at 1273 K (Figure 10d). Hence, again a substantial part of the chromium content in this material is present at low thermal treatment temperatures in the 6+ oxidation state.

(32) Kutzler, F. W.; Natoli, C. R.; Misemer, D. K.; Doniach, S.; Hodgson, K. O. *J. Chem. Phys.* **1980**, *73*, 327.
(33) Penner-Hahn, J. E.; Benfatto, M.; Hedman, B.; Takahashi, T.; Doniach, S.; Groves, J. T.; Hodgson, K. O. *Inorg. Chem.* **1986**, *25*, 2255.
(34) Wong, J.; Lytle, F. W.; Messmer, R. P.; Maylotte, D. H. *Phys. Rev. B* **1984**, *30*, 5596.
(35) Hawkins, J. K.; Isaacs, H. S.; Heald, S. M.; Tranquada, J.; Thompson, G. E.; Wood, G. C. *Corrosion Sci.* **1987**, *27*, 391.
(36) Miyake, M.; Nakgawa, N.; Ohyanagi, H.; Suzuki, T. *Inorg. Chem.* **1986**, *25*, 700.

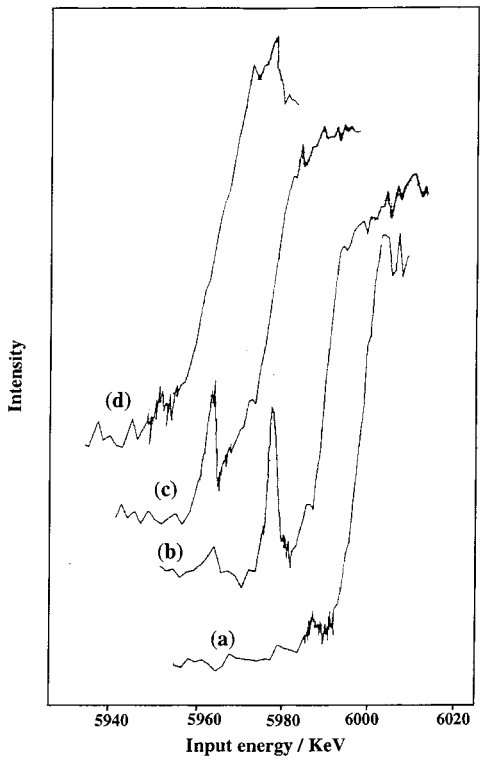

Figure 9. Cr K X-ray absorption edge of the Cr(III)/CeO_2-imp (Cr:Ce 0.06) material calcined at (a) 383 K, (b) 573 K, (c) 873 K, and (d) 1273 K.

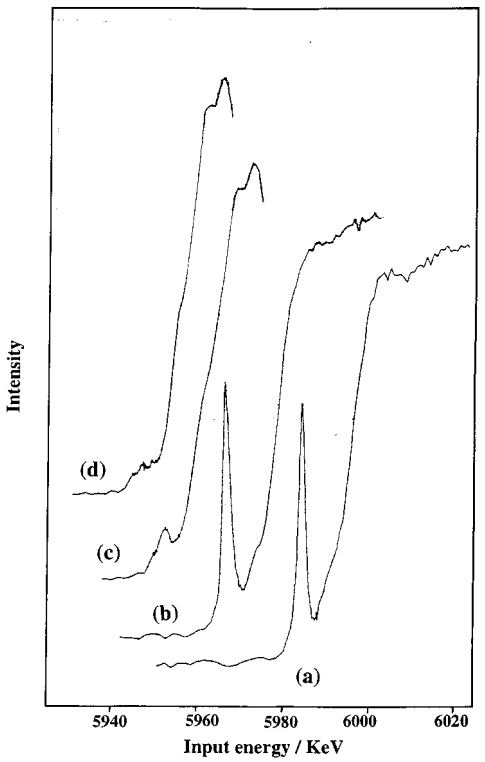

Figure 10. Cr K X-ray absorption edge of the Cr(III)/CeO_2-cop (Cr:Ce 0.06) material calcined at (a) 383 K, (b) 573 K, (c) 873 K, and (d) 1273 K.

Figure 11 shows a plot of the variation of the peak intensity of the pre-edge feature with calcination temperature for all three types of material. From this it can be seen that thermal processing at 573 K, the conditions that produce that most active catalyst, induces a substantial quantity of chromium in the 6+ oxidation state, irrespective of the oxidation state of the chromium precursor employed.

Electron Paramagnetic Resonance. Studies by Weckhuysen et al.[37,38] on Cr(VI)/SiO_2 and Cr(VI)/Al_2O_3 catalysts have shown that three different chromium signals are observable in the EPR depending on the treatment history of the catalysts. These are referred to as the δ-, γ-, and β-signals. The δ- and β-signals are broad and occur in the g_{eff} ranges ca. 5 and 1.96−2.45, respectively. The δ-signal results from dispersed Cr^{3+} ions whereas the β-signal is assigned to clusters of Cr^{3+}. The β-signal is strongly dependent on the size and shape of these clusters as indicated by the broad range of g values. The γ-signal is much sharper and occurs at $g = 1.97$. The assignment of the γ-signal is the source of much contention. Spitz[39] has attributed the signal to mixed-valence trimers, $Cr^{VI}-O-Cr^{III}-O-Cr^{VI}$, with an average Cr oxidation state of 5+. This assignment has been supported by other authors working on alumina-[40] and titania-supported[41] chromium oxide catalysts. However, an alternative interpretation assigns the signal to a mononuclear chromyl (Cr^{V}) complex with square pyramidal coordination, which is stabilized by interaction with the support surface. This has been proposed by EPR studies of the Cr/ZrO_2[41] and Cr/SiO_2/Al_2O_3[36] systems.

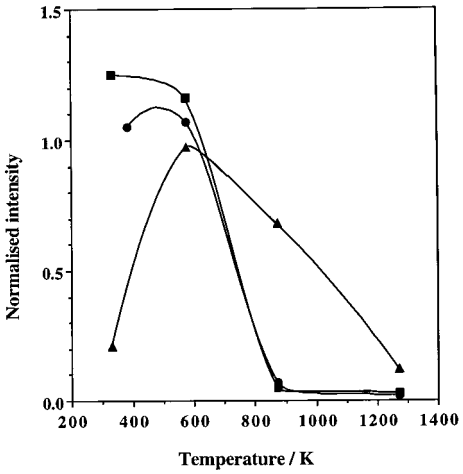

Figure 11. Plot of the variation of the peak intensity of the pre-edge feature with temperature for Cr(III)/CeO_2-imp (▲), Cr(III)/CeO_2-cop (●), and Cr(VI)/CeO_2-imp (■) materials.

EPR spectra taken of the Cr(III)/CeO_2-imp (Cr:Ce 0.06) material calcined at temperatures in the range 333−1273 K are shown in Figure 12. The spectrum of the material dried at 333 K comprises two Cr signals: a broad, isotropic ($g_{iso} \approx 2$) peak centered at ca. 3500 G ($\Delta H \approx 350$ G) on which is superimposed a sharper, intense line ($g_\perp = 1.972$, $g_\parallel = 1.945$). In line with previous work,[36,37] these two signals are assigned as β- and γ-signals, respectively. The broader β-signal is assigned to Cr^{3+} with near octahedral coordination,

(37) Weckhuysen, B. M.; Schoonheydt, R. A.; Mabbs, F. E.; Collison, D. *J. Chem. Soc., Faraday Trans. 1* **1996**, *92*, 2431.
(38) Weckhuysen, B. M.; De Ridder, L. M.; Grobert, P. J.; Schoonheydt, R. A. *J. Phys. Chem.* **1995**, *99*, 320.
(39) Spitz, R. *J. Catal.* **1974**, *35*, 345.
(40) Ellison, A.; Singh, K. S. W. *J. Chem. Soc., Faraday Trans.* **1977**, *73*, 2807.
(41) Amorelli, A.; Evans, J. C.; Rowlands, C. C.; Egerton, T. A. *J. Chem. Soc., Faraday Trans.* **1987**, *83*, 3541.

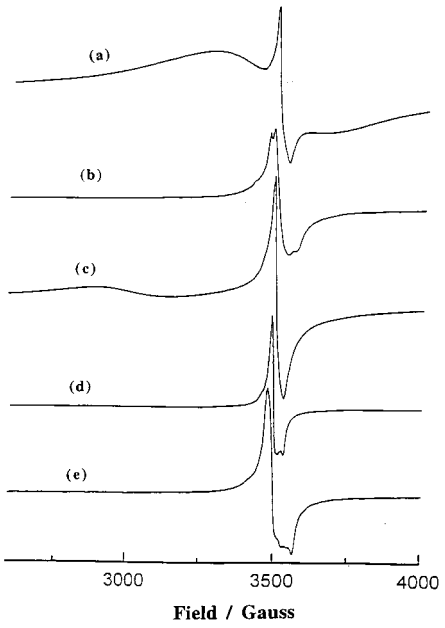

Figure 12. EPR spectra of the Cr(III)/CeO_2-imp (Cr:Ce 0.06) material calcined at (a) 333 K, (b) 573 K, (c) 873 K, (d) 1073 K, and (e) 1273 K.

most probably hexa-aqua ions that are adsorbed onto the ceria surface during impregnation. Because in this sample the X-ray absorption spectra show that no Cr(VI) (and hence no mixed-valence species) is present after drying at 333 K, the γ-signal in the spectrum (5× magnification) of this material is assigned to a surface-supported chromyl (Cr^V) species. Calcination at 573 K causes an increase in intensity of the γ-signal, which is consistent with the formation of a mixed-valence species also indicated by the formation of substantial quantities of Cr(VI) observed by X-ray absorption. This signal is superimposed on the now much narrower β-signal ($g_{iso} \approx 1.98$, $\Delta H = 100$ G) assigned to clustered Cr(III) cations (or possibly an amorphous Cr_2O_3 phase). Upon calcination at 873 K, the intensity of the γ-signal is reduced (3× magnification), suggesting the destruction of the mixed-valence species. Calcination at 1073 and 1273 K leads to further loss of intensity in the γ-signal. Because it is unlikely that mixed-valence species survive at these temperatures, the signal is assigned to isolated Cr(V) ions, which are supported by strong interactions with the ceria surface. Cimino et al.[41] have reported the stability of such complex ions supported on zirconia at temperatures up to 1173 K.

EPR spectra of the Cr(III)/CeO_2-cop (Cr:Ce 0.06) material dried at 383 K comprises an intense γ-signal (centered at 3450 G), which because the X-ray absorption spectrum indicates substantial Cr(VI) we assign to a mixed-valence Cr(III)/Cr(VI) species, although the presence of some Cr(V) cannot be excluded. The spectrum of material calcined at 573 K contains a broad peak that is the superposition of the γ- ($g_\perp = 1.966$, $g_{||} = 1.941$, $\Delta H = 40$ G) and β-signals. The latter ($g_{iso} \approx 1.98$) is assigned to Cr(III) in small clusters,[42] which increase in size upon further calcination. Calcination at 873 K and above causes a decrease in intensity of the γ-signal, leading to the destruction of the mixed-valence species and growth of crystalline Cr_2O_3. The β-signal is still evident at these higher temperatures, though its intensity is low due to the effects of antiferromagnetic coupling.

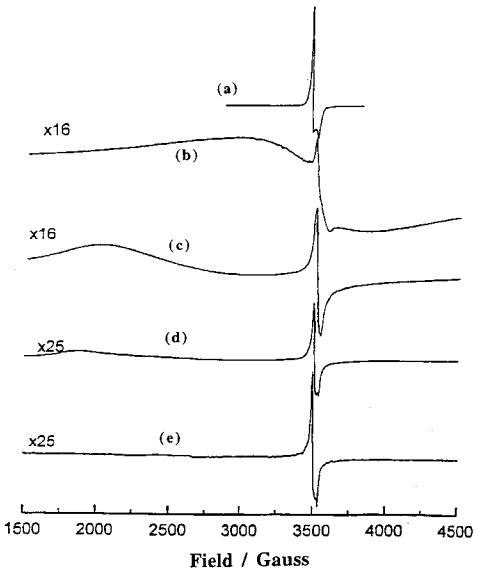

Figure 13. EPR spectra of the Cr(VI)/CeO_2-imp (Cr:Ce 0.07) material calcined at (a) 333 K, (b) 573 K, (c) 873 K, (d) 1073 K, and (e) 1273 K.

Figure 13 shows the EPR spectra of Cr(VI)/CeO_2-imp (Cr:Ce 0.07) material calcined for 16 h in the temperature range 333−1273 K. The presence of an EPR signal in the spectrum of the material dried at 333 K is surprising because Cr(VI) ($3d^0$) is EPR silent. Because it is unlikely that reduction of Cr(VI) to Cr(III) has taken place in this sample at this stage (and thereby creating a mixed-valence species), the γ-signal ($g_\perp = 1.965$, $g_{||} = 1.936$) in this spectrum is assigned to a Cr(V) species. A second $g_{||}$ line in the signal suggests that a rhombic, as opposed to axial, symmetry may be adopted by this Cr(V) species on the ceria surface. Extrapolating from the intensity of the X-ray absorption pre-edge data shown in Figure 8, the amount of chromium(VI) reduced is estimated to be only 8.1% of the total chromium content.

Calcination at 573 K leads to the appearance of a broad ($\Delta H \approx 800$ G) β-signal ($g_{iso} \approx 1.98$), indicative of Cr(III) clusters, and it is probable that the γ-signal is due to the formation of a mixed-valence species rather than Cr(V). The intensity of the γ-signal decreases upon calcination at 873 K through loss of the mixed-valence species. The appearance of a signal at ca. 2000 G is due to the Cr δ-signal ($g_{eff} = 4.5$), indicative of dispersed Cr^{3+} ions in distorted octahedral coordination.[36] Calcination at higher temperatures causes further reduction of intensity in the γ-signal and the loss of Cr(III) signals. This is due to antiferromagnetic coupling, which occurs in the Cr_2O_3 crystalline phase present at this temperature.

EPR Studies of Surface Redox Reactions. The surface redox chemistry of the Cr(III)/CeO_2-imp and Cr(VI)/CeO_2-imp materials after calcination at 673 K were investigated by dosing the materials using a CO atmosphere followed by subsequent reoxidation of the material by O_2.

After this thermal treatment the spectrum of the Cr(III)/CeO_2-imp material comprises an intense peak at

(42) Köhler, K.; Schläpfer, C. W.; Engweiler, J.; Baiker, A. *J. Catal.* **1993**, *143*, 201.

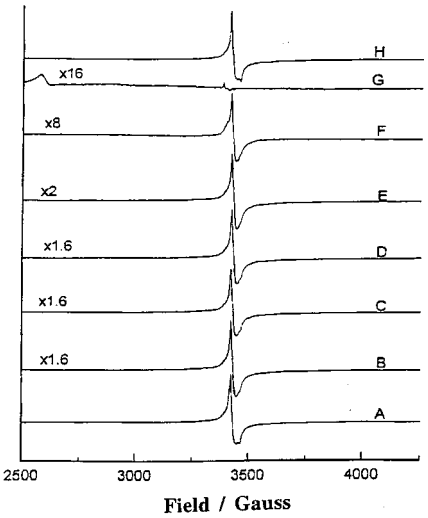

Figure 14. EPR spectra of the CO reduction and subsequent reoxidation of the Cr(III)/CeO_2-imp (Cr:Ce 0.06) material calcined at 673 K. See text for details of treatments.

ca. 3450 G, which is the superimposition of the β- and γ-signals due to small Cr(III) clusters and the mixed-valence Cr^{III}/Cr^{VI} species, respectively (Figure 14A). The intensity of this signal is unchanged by thermal treatment (in vacuo) at 573 K (Figure 14B) or by exposure to 400 Torr CO at 298 K (Figure 14C). No change is apparent upon raising the temperature to 323 K (Figure 14D), with the sample still under 400 Torr CO, although a slight decrease in signal intensity does occur upon heating at 373 K (Figure 14E). Increased thermal treatment under the CO atmosphere at 473 K (Figure 14F) brings about both a significant decrease in signal intensity and a broadening of the signal corresponding to the reduction of Cr(VI) in the sample to Cr(III) and the ensuing loss of mixed-valence $Cr^{VI}-Cr^{III}-Cr^{VI}$ species. Treatment at 573 K (Figure 14G) brings about the complete reduction of Cr(VI) and the removal of the γ-signal. A low-field δ-signal at ca. 2600 G is indicative of isolated Cr^{3+} ions. Complete reoxidation of the sample and restoration of the original signal (Figure 14H) is achieved by thermal treatment (at 673 K) under 400 Torr O_2 for 1 h.

The changes in the spectra of the Cr(VI)/CeO_2-imp material calcined at 673 K when exposed to an atmosphere of CO, and the subsequent reoxidation by O_2, are illustrated in Figure 15. The spectrum of the material calcined ex situ at 673 K (Figure 15A(i)) exhibits both δ- and γ-signals attributed to dispersed Cr^{3+} ions and the mixed-valence Cr^{VI}/Cr^{III} species, respectively. No changes were apparent when the material was subjected to evacuation at 573 K, and very little change was observed when the sample was exposed to an atmosphere of carbon monoxide at temperatures up to 373 K. However, treatment at 473 K caused the intensity of the γ-signal to be reduced drastically (Figure 15A(vi)), and at 573 K the γ-signal was essentially absent (Figure 15A(vii)).

The reoxidation of the reduced material through thermal treatment under an O_2 atmosphere is illustrated in Figure 15B. After the sample was allowed to cool, 400 Torr of O_2 was admitted to the cell at ambient temperature (298 K) and heated in stages (0.5 h exposure times). The regeneration of the γ-signal

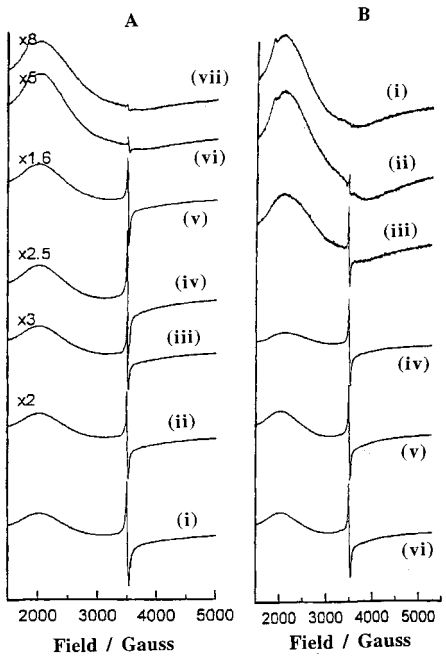

Figure 15. EPR spectra of (A) the CO reduction and (B) the reoxidation of the Cr(VI)/CeO_2-imp (Cr:Ce 0.07) material calcined at 673 K. (A) (i) The EPR spectrum of the material after ex situ calcination at 673 K, (ii) after evacuation treatment at 573 K, and (iii) after exposure to 400 Torr CO at 298 K, (iv) 323 K, (v) 373 K, (vi) 473 K, and (vi) 573 K. (B) (i) The spectrum after reduction by CO followed by cooling to ambient temperature followed by exposure to 400 Torr O_2 at 373 K (ii), 473 K (iii), 573 K (iv), 673 K (v) and 773 K (vi).

begins at 373 K, and complete reoxidation is achieved after treatment at 773 K.

Discussion

Preparative Route and the Nature of the Catalytic Materials. Three methods may be employed to prepare chromium-promoted ceria catalysts:

(i) impregnation of CeO_2 using aqueous CrO_3 solutions,

(ii) impregnation of CeO_2 using aqueous chromium(III) nitrate solutions;

(iii) coprecipitation from aqueous solutions containing both cerium(IV) and chromium(III) ions.

The freshly prepared gel materials all comprise small (ca. 1−2 nm) particles. When route (i) is employed, chromate(VI) anions (principally dichromate together with small amounts of monochromate and trichromate) are sorbed onto the surface of these particles. The nature of the chromium species in the materials obtained by routes (ii) and (iii) are most probably sorbed $\{Cr(H_2O)_6^{3+}\}$ cations and polymeric γ-CrO(OH), respectively. The chromium loading by sorption methods (routes (i) and (ii)) can be controlled by careful control of the experimental variables, affording a high degree of reproducibility, and the relationship between chromium loading and molarity of the aqueous CrO_3 solution is shown in Figure 1. The chromium content of catalyst materials produced by the coprecipitation method (route (iii)) is usually only about half that expected from the Cr:Ce ratio in the aqueous solution prior to precipitation.

Optimum catalytic performance of chromium-promoted ceria materials is achieved after thermal activa-

tion in air in the temperature range 573−673 K. After such treatment the catalytic activity is similar, irrespective of whether the source of the chromium promoter is in oxidation state 3+ or 6+. It is notable that increasing chromium loading lowers the temperature for complete conversion of propane, but has a detrimental effect for the conversion of CO, increasing the T_{100}(CO) temperature. In fact, the efficacy of the Cr/CeO_2 materials in catalyzing the CO oxidation reaction is approximately the same as that of unpromoted CeO_2 and vastly inferior to Cu/CeO_2 catalyst materials.[21] Thermal treatment at more elevated temperatures results in a progressive lowering of activity for all materials. However, it is notable that 100% conversion of propane is still achieved ($T_{100}(C_3H_8)$ 763 K), even after calcination at 1273 K.

The key issues for these catalyst materials are (i) what is the nature of the materials after thermal activation processing, (ii) does the preparative route play any role, (iii) what is the nature of the chromium promoter, (iv) how do the materials change upon thermal processing at elevated temperatures, and (v) how do the materials function in the catalytic processes?

All three types of materials appear to have a very similar constitution after thermal processing in the temperature range 573−673 K, that necessary for optimum catalytic performance. XRD indicates only the presence of microcrystalline ceria particles ca. 3 nm in size with the chromium component being amorphous. In addition, infrared data indicate the presence of Cr(VI)−O stretching modes and X-ray absorption spectra exhibit strong pre-edge features also indicative of chromium(VI). However, the EPR spectra for both the $Cr(III)/CeO_2$-cop and $Cr(VI)/CeO_2$-imp materials calcined at this temperature exhibit β- and γ-signals due to small Cr(III) oxide-like clusters and a mixed-valence Cr^{III}/Cr^{IV} species, respectively. Similar data are also obtained for the $Cr(III)/CeO_2$-cop material calcined at the much lower temperature of 383 K, whereas under the same conditions the $Cr(III)/CeO_2$-imp material exhibits no evidence for chromium(VI), although not surprisingly the $Cr(VI)/CeO_2$-imp material does.

Hence, we infer that the nature of the catalysts formed by thermal processing of the initial materials formed by all three routes in the temperature range 573−673 K is essentially the same, irrespective of whether the source of the chromium promoter is in oxidation state 3+ or 6+. This also rationalizes the apparent lack of dependence of the catalytic activity on the preparative route as also observed for analogous Cr/SnO_2 catalysts.[43] Further, we might speculate that the nature of the catalyst materials in the present case is possibly similar to that found for the Cr/SnO_2 catalysts,[44] i.e., the mixed-valence compound Cr_5O_{12} supported on particulate ceria, although other mixed-valence compounds such as oxides including Cr_3O_8 and Cr_2O_5 must also be considered possible. That the constitution is not as simple as this is demonstrated by the EPR data, which also shows the presence of Cr(III) oxide-like clusters. We, therefore, propose that the active catalyst is a composite oxide material comprising microparticulate mixed-valence chromium Cr^{III}/Cr^{VI} species (which could be Cr_5O_{12}) together with Cr(III) oxide-like clusters dispersed on particulate ceria.

Thermal processing at 873 K results in significant reduction of the chromium(VI) component in all three types of material. XRD shows the presence of ceria particles <10 nm in size together with larger (14.5 nm) phase-separated Cr_2O_3. However, again EPR shows that the true situation is more complex, with signals due to either Cr(III) oxide-like clusters ($Cr(III)/CeO_2$-cop and $Cr(III)/CeO_2$-imp materials) or dispersed or isolated Cr(III) ions (the $Cr(VI)/CeO_2$-imp material). After calcination at 1273 K, all the catalyst materials comprise a particulate composite of CeO_2 and Cr_2O_3 crystallites, both ca. 100 nm in size.

The mechanism by which the active catalyst materials are formed is obviously very complex. Even the thermal decomposition of pure chromium compounds in both the 3+ and 6+ oxidation states involve several stages with a number of intermediates. Hydrous chromium(III) oxide prepared by precipitation from aqueous solution undergoes only dehydration, albeit in several stages before eventually forming α-Cr_2O_3.[45,46] Decomposition of chromium(III) nitrate hydrate, $Cr(NO_3)_3{\cdot}9H_2O$, at 573 K affords poorly crystallized α-Cr_2O_3 with minority bulk and surface Cr^{4+} and Cr^{6+} species, showing that some oxidation of the chromium(III) to higher oxidation states (presumably by nitrate) can occur. At higher temperatures well-crystallized α-Cr_2O_3 with surface chromates is formed.[47]

Crystalline Cr_5O_{12} is formed in the thermal decomposition of CrO_3 but the conditions need to be controlled carefully (temperature range 513−533 K, oxygen pressures in the range 2−3 kbar, 3−7 days)[48] and is better represented as $Cr^{III}_2(Cr^{VI}O_4)_3$. Under ambient pressure the thermal decomposition of neat CrO_3 is reported to start at its melting point (470 K), but if the compound is heated above ca. 493 K, oxygen is lost stepwise to form a succession of lower oxides including Cr_3O_8, Cr_2O_5, and CrO_2 until the eventual formation of α-Cr_2O_3 at ca. 720 K.[49,50]

The thermal decomposition behavior of $Cr(NO_3)_3{\cdot}9H_2O$ and CrO_3 supported on silica and alumina behave in a broadly similar fashion to the behavior of unsupported compounds.[6,47,51] The oxidation of Cr(III) to Cr(VI) is initiated near 473 K and involves stepwise oxidation by atmospheric oxygen. However, in the presence of an active oxidant (such as NO_3^- ions), oxidation is greatly enhanced and commences at temperatures below 473 K. On the other hand, in a reducing atmosphere reduction of Cr(VI) to Cr(III) can also take place in the region of 473 K, though temperatures of >673 K are typically required in an O_2-rich environment. At 573 K $Cr(III)/SiO_2$ and $Cr(VI)/SiO_2$ materials afford poorly crystallized supported chromium oxides of stoichiometries $CrO_{2.1}$ and $CrO_{2.6}$, respectively, whereas

(43) Harrison, P. G.; Bailey, C.; Azelee, W. *J. Catal.* **1999**, *186*, 147.
(44) Harrison, P. G.; Lloyd, N. C.; Daniell, W.; Bailey, C.; Azelee, W. *Chem. Mater.* **1999**, *11*, 896.
(45) Singh, K. K.; Sarade, P. R.; Ganguly, P. *J. Chem. Soc., Dalton Trans.* **1983**, 1895.
(46) Spiccia, L.; Marty, W.; Giovanoli, R. *Helv. Chim. Acta* **1987**, *70*, 1737.
(47) Fouad, N. E.; Knözinger, H.; Zaki, M. I. *Z. Phys. Chem.* **1994**, *186*, 231.
(48) Wilmhelmi, K. A. *Acta Chem. Scand.* **1965**, *19*, 165.
(49) Kubota, B. *J. Am. Ceram. Soc.* **1961**, *44*, 239.
(50) Fouad, N. E. *J. Therm. Anal.* **1996**, *46*, 1271.
(51) Fouad, N. E.; Knözinger, H.; Ismail, H. M.; Zaki, M. I. *Z. Phys. Chem.* **1991**, *173*, 201.

at 873 K large crystallites of α-Cr_2O_3 are formed in both cases. The only effect of the silica support appears to be the formation of smaller chromium oxide particle sizes. No crystalline chromia species were formed on alumina as a support material irrespective of calcination temperature, although very weak X-ray diffraction features of α-Cr_2O_3 are observed at 873 K. The stoichiometry of the chromium oxide species formed on alumina is independent of the oxidation state of the chromium source and is determined only by the temperature of calcination, a stoichiometry of $CrO_{2.2}$ being formed at 573 K and $CrO_{1.7-1.8}$ being formed at 873 K. It would appear, therefore, that the predominant species formed on alumina after calcination at 573 K is chromium(IV) oxide, CrO_2. In a separate study the formation of Cr_5O_{12} clusters have been proposed upon heating of Cr(VI)-promoted silica to 573 K.[52]

Partial oxidation of Cr(III) to Cr(VI) has previously been reported for Cr(III)-promoted titania.[27] Oxidation begins at temperatures as low as 373−413 K and that both Cr(VI) and Cr(III) are present at these temperatures. Whether this oxidation involves the formation of mononuclear or polynuclear chromate ions or the partial oxidation (and agglomeration) of hydrated surface-bound Cr(III) ions to form a mixed-valence Cr^{VI}/Cr^{III} oxide phase is a matter of much contention. At temperatures in the region of 573−673 K, however, reduction of Cr(VI) occurs (even under oxidizing conditions), which leads to the formation of crystalline chromium(III) oxide at 873 K. EXAFS studies show that Cr(III)-containing pillared clay catalysts behave similarly and indicate that Cr_5O_{12} is formed upon calcination at 523 K.[53]

Compared to alumina or silica, ceria is a relatively oxidizing medium, and it is not too surprising that chromium(III) species in ceria undergo transformation to higher oxidation states. What is perhaps surprising is the formation of chromium(VI) in the Cr(III)/CeO_2-cop material, but not in the Cr(III)/CeO_2-imp material, under mild (383 K) thermal-processing conditions, and this is probably due to the intimate mixing of cations at the atomic level.

Catalytic Reaction Mechanisms. Several conclusions concerning the mechanistic pathways may be drawn from the present study: (a) thermal processing in the temperature range 573−673 K produces optimum catalytic performance for the oxidation of both carbon monoxide and propane, (b) thermal processing at higher temperaures results in lower performance and higher T_{100} values for both, (c) 100% conversion of propane is still achieved, even after thermal processing at 1273 K, (d) the active catalyst after processing at 573−673 K appears to be a composite of microparticulate ceria with a mixed-valence Cr^{VI}/Cr^{III} chromium species, probably Cr_5O_{12}, as well as some chromium(III) oxide-like species, essentially irrespective of the preparative route, (e) after thermal processing at temperatures ≥873 K the materials comprise a composite of microparticulate ceria and Cr_2O_3, (f) the mixed-valence component of the catalyst undergoes facile reduction upon exposure to carbon monoxide at 473−573 K and is reoxidized upon exposure to oxygen at the same temperature, and (g) promotion of ceria by chromium significantly enhances activity toward the oxidation of propane, but has only a marginal effect on the oxidation of carbon monoxide.

The oxidation of CO over promoted metal oxide catalysts is an area of catalysis that has been the center of discussion for many years, producing numerous and often conflicting models and mechanisms. The main areas of contention include (i) the role of the metal promoter or promoters, (ii) the role of the metal oxide support, (iii) the interaction between promoter and support (if any), (iv) the active sites for CO and O_2 adsorption, and finally, (v) the mechanism itself. The latter is in its own right a matter of much debate, with theories ranging from an Eley−Rideal-type reaction mechanism, where the rate-determining step is the adsorption of CO molecules onto a metal surface[54] (which itself is dispersed over the surface of the metal oxide support), to a Langmuir−Hinshelwood mechanism involving adsorption of CO onto dispersed metal particles and reaction with oxygen activated on the oxide surface as superoxide ions (O_2^-)[55] or extracted from the oxide lattice (Mars van Krevelen mechanism), leaving behind lattice oxygen vacancies.[56] It is this latter mechanism that is believed to be adopted for oxidation over promoted ceria catalysts, taking advantage of the known oxygen storage capacity of the material.[57]

After thermal processing at temperatures as low as 673 K, ceria itself is fully capable of facilitating the oxidation of carbon monoxide without the aid of promoters. Oxidation is considered to occur through adsorption of CO (most likely on Ce^{4+} Lewis acid sites exposed on the surface) and extraction of oxygen from the ceria lattice,[58] creating lattice oxygen vacancies and the subsequent reduction of neighboring Ce^{4+} ions to Ce^{3+}. Adsorption of oxygen regenerates the lattice oxygen sites, reoxidizing the metal ions to Ce^{4+}. Promotion of ceria with copper(II) enhances the activity toward the oxidation of carbon monoxide dramatically.[21] The mode of action of such Cu(II)/CeO_2 catalyst materials appears to be synergistic in nature with the principal role of Cu(II) being mainly in electron transfer, abstracting the negative charge remaining when oxygen vacancies are formed following desorption of CO_2. The significant enhancement of catalytic activity is due in large part to the efficiency of the Cu(II)/Cu(I)[21] (or Cu(I)/Cu(0)[55]) couple in this process. That the presence of chromium in the catalyst does not enhance the activity toward CO oxidation above that of ceria itself is probably due to its inability to perform the same role as copper. However, the activity of Cr/SiO_2 and Cr/Al_2O_3 materials has been attributed to the presence of the Cr^{3+}/Cr^{6+} redox couple, and the oxidation of CO over material containing the mixed-valence species was oberved to occur faster than that over samples in which only Cr^{3+} was present.[6,47]

Mixed-valence Cr^{III}/Cr^{VI} clusters are also probably involved in the oxidation of propane over these Cr/CeO_2

(52) Ellison, A.; Diakun, G.; Worthington, P. *J. Mol. Catal.* **1988**, *46*, 131.
(53) Corker, J. M.; Evans, J.; Rumney, J. M. *Mater. Chem. Phys.* **1991**, *29*, 201.
(54) Choi, K. I.; Vannice, M. A. *J. Catal.* **1991**, *131*, 22.
(55) Liu, W.; Flytzani-Stephanopoulos, M. *J. Catal.* **1995**, *153*, 317.
(56) Breysse, M.; Guenin, M.; Claudel, B.; Latreille, H.; Veron, J. *J. Catal.* **1972**, *27*, 275.
(57) Cho, B. K.; Shanks, B. M.; Bailey, J. E. *J. Catal.* **1989**, *115*, 486.
(58) Li, C.; Xin, Q. *J. Phys. Chem.* **1992**, *96*, 7714.

catalysts. Methane oxidation activity over alumina-supported chromia has been reported to increase with an increased number of Cr^{III}/Cr^{VI} clusters present on the surface. However, at high chromium loadings activity is low due to Cr_2O_3 formation.[14] Agglomerates of Cr_2O_3 seriously reduce the activity of supported chromia catalysts toward the oxidation of isobutane, where the active sites were proposed to be dispersed $Cr^{VI}O_x$ species.[10] In the present case the catalytic oxidation of propane must proceed by initial adsorption of propane molecules on to the catalyst surface. Liu et al.[58] have proposed that, for methane oxidation over ceria, this probably takes place on surface coordinately unsaturated oxygen (Lewis base) sites. The second step involves the activation of C−H bonds and formation of surface formates, which then decompose into smaller fragments such as carbonates, before finally desorbing from the surface as CO_2 and water.[59] The high activation energy of the reaction is associated with the breaking of C−H and C−C bonds. Chromium-promoted tin(IV) oxide catalysts also facilitate the catalytic oxidation of propane, with complete conversion ocurring at temperatures in the range 583−653 K,[43] somewhat higher than those observed for the Cr/CeO_2 catalysts in the present study.

The initial step of adsorption of propane to the catalyst surface is necessarily one involving hydrogen abstraction by surface nucleophilic oxygen and the formation of surface hydroxyl and alkoxy groups. The prime candidate for this is the highly nucleophilic chromyl Cr(VI)═O oxygen present in the mixed-valence species formed after thermal processing at 573−673 K. We have shown previously that, for materials based on tin(IV) oxide, surface-adsorbed alkoxy groups are readily converted via surface carboxylates and carbonates to carbon dioxide.[60] Due to the similarity of oxidizing characteristics of tin(IV) oxide and ceria, we propose that a similar pathway is followed in the present case.

Thermal processing at temperatures ≥873 K results in an increase in the T_{100} temperature for both catalytic reactions. This temperature coincides with two major changes in the catalyst material: (a) the mixed-valence component is transformed into Cr_2O_3, which phase separates at high temperatures, and (b) the crystallite size and both CeO_2 and Cr_2O_3 components increase rapidly. An increase in particle size is accompanied by a decrease in surface area and surface sites available for adsorption and reaction, leading to a lowering of activity. That the surface area of metal oxide catalyst materials such as these falls quite dramatically after thermal processing at temperatures in excess of 873 K is well documented.[10,34] Transformation of the mixed-valence component into Cr_2O_3 removes the nucleophilic Cr(VI)═O sites necessary for propane adsorption, which also will reduce activity. It is interesting to note that even after thermal processing at 1273 K the Cr/CeO_2 catalyst still gives 100% conversion of propane (T_{100} 763 K). At this temperature the catalyst comprises essentially a *physical composite mixture* of CeO_2 and Cr_2O_3 crystallites both ca. 100 nm in size.

Conclusions

Three methods may be employed to prepare chromium-promoted ceria catalysts: (i) impregnation of CeO_2 using aqueous CrO_3 solutions, (ii) impregnation of CeO_2 using aqueous chromium(III) nitrate solutions, and (iii) coprecipitation from aqueous solutions containing both cerium(IV) and chromium(III) ions. However, the nature of the freshly prepared gel materials is different in each case. All comprise small (ca. 1−2 nm) particles of hydrous ceria on the surface of which are sorbed chromate(VI) anions (route (i)), $\{Cr(H_2O)_6^{3+}\}$ cations (route (ii)), or polymeric γ-CrOOH (route (iii)) depending on the preparative route.

Thermal processing in the temperature range 573−673 K produces optimum catalytic performance for the oxidation of both carbon monoxide and propane irrespective of whether the source of the chromium promoter is in oxidation state 3+ or 6+. The active catalyst appears to be a composite of microparticulate ceria with a mixed-valence Cr^{VI}/Cr^{III} chromium species, probably Cr_5O_{12}, as well as some chromium(III) oxide-like species. Thermal processing at higher temperatures results in lower performance and higher T_{100} values for both.

The mixed-valence component of the catalyst undergoes facile reduction upon exposure to carbon monoxide at 473−573 K and is reoxidized upon exposure to oxygen at the same temperature. The mechanism of propane oxidation most probably involves adsorption of propane to the catalyst surface at the highly nucleophilic chromyl Cr(VI)═O oxygen present in the mixed-valence species, resulting in hydrogen abstraction and the formation of surface hydroxyl and alkoxy groups.

The decrease in catalytic activity at temperatures ≥873 K is probably due to the transformation of the mixed-valence component into Cr_2O_3, which phase separates at high temperatures. Nevertheless, the Cr/CeO_2 catalyst still gives 100% conversion of propane (T_{100}, 763 K), even after thermal processing at 1273 K when the catalyst comprises essentially a *physical composite mixture* of CeO_2 and Cr_2O_3 crystallites both ca. 100 nm in size.

Acknowledgment. We thank the Commission of the European Community (Contract AVI* CT92 − 0012) and the EPSRC (for Research Grant GR/J76026 and providing facilities at DRAL) for support.

CM001193S

(59) Li, C.; Xin, Q.; Guo, X.; Onishi, T. *Stud. Surf. Sci. Catal.* **1993**, *75*, 1955.

(60) Harrison, P. G.; Maunders, B. *J. Chem. Soc., Faraday Trans. 1* **1985**, *81*, 1311, 1329, 1345.